INNOVATIVE MECHANICAL ENGINEERING **ISSN 2812-9229 (Online)**
University of Niš, Faculty of Mechanical Engineering
VOL. 1, NO 3, 2022, PP. 10 - 20

Original scientific paper *

IMPACT OF NONLINEARITY ON RF ENERGY HARVESTER IN IOT RELAY SYSTEMS

Aleksandra Cvetković[1], Vesna Blagojević[2], Maša Milošević[1], Jelena Manojlović[1]

[1]University of Niš, Faculty of Mechanical Engineering, Niš, Serbia

[2]University of Belgrade, School of Electrical Engineering

Abstract. *This paper presents the analysis of the scenario where a relay node is used to enable communication between a source and an Internet of Things (IoT) edge node. The position of the relay is set to provide line-of-sight communication between the source and the relay node while communication in the relay-IoT edge link is still jeopardized by obstacles. As the relay node is energy limited, it is powered by RF energy from the source based on a time-switching protocol. Assuming that the energy harvester is a nonlinear device, the impact of nonlinearity, channel and system parameters on outage system performance is investigated and discussed.*

Key words: *IoT relay system, Nonlinear harvester, Outage performance, RF Energy harvesting, Time switching protocol.*

1. INTRODUCTION

The rapid growth of devices that are used in everyday life to improve its quality (in the concepts such as smart home, smart grid, smart city...) has led to the increased energy consumption [1]. On the other hand, numerous Internet of Things (IoT) devices used for monitoring environmental parameters or monitoring in industry require efficient power in order to enable high energy efficiency and alleviate potential environmental problems [2]. The usage of technologies for energy harvesting from various natural energy sources such as solar, thermal or wind power, can lead to a prolonged battery lifetime. These power supply techniques are environmentally friendly, but represent time-varying power sources, dependent on the weather conditions [3].

The usage of radio frequency (RF) signals, which can be employed to transfer both information and energy, is one of the most effective methods for powering wireless devices [3, 4]. RF waves are constantly present in most of environments and therefore they provide

*Received: December 13, 2022 / Accepted December 27, 2022.
Corresponding author: **Aleksandra Cvetković**
Institution : Faculty of Mechanical Engineering, University of Niš, Serbia
E-mail: aleksandra.cvetkovic@masfak.ni.ac.rs

a stable and efficient solution for supplying energy to low-power devices [2-7]. The technique of simultaneous wireless transfer of information and power (SWIPT) can be applied in an IoT network for both relay and sensor nodes, providing coverage of large areas and enabling the same quality of service for all nodes. In order to achieve required high data rates, as well as to mitigate wireless channel impairments, the additional (relay) node between the source and the destination node may be used. Those schemes are well-known as a cooperative relay scheme [6-7].

The analysis of the SWIPT concept is given in [8], while the practical receiver design for concurrent transfer of information and energy is considered in [9]. The protocols for the transmission of information and energy signals in a cooperative relay network are proposed in [10]: time-switching relaying (TSR) protocol and power-splitting relaying (PSR) protocol. In the TSR-based scheme, one part of time is used to harvest energy at the relay, while the rest of it is dedicated to decoding and transmission. On the other hand, in the PSR-based receiver architecture, one part of received power is utilized for harvesting, while the remaining power is used for signal processing [10]. Cooperative relaying systems with the application of SWIPT for both TSR and PSR protocols in Rayleigh and Nakagami-*m* fading environment are analyzed in [11] and [12], respectively. The impact of the line-of-sight (LoS) component in the amplify-and-forward SWIPT relaying system is analyzed in [13], while the analysis of the decode-and-forward system is provided in [14]. The system performance analyses for both TSR and PSR protocols in the Generalized-*K* fading environment is presented in [15].

The linear energy harvester model was considered in all previously mentioned papers. Although this approach is useful, it has been observed that practical harvesters suffer from nonlinear behavior because of the nonlinearities of the electrical components [16,17]. The analysis of a network with a nonlinear harvester in the Nakagami-m fading environment is presented in [18] and [19]. In this paper we provide outage performance analysis of the relaying system with the nonlinear energy harvester in the environment where the LoS component exists between the source and the relay node, while the link between the relay and the IoT edge node is suffering from both fading and shadowing due to many obstacles. This paper analyzes the application of RF energy harvesting technology in cooperative wireless IoT networks, combining high reliability and spectral efficiency offered by cooperative transmission, with modern energy-efficient and flexible solutions for powering devices.

2. System and channel model

We assume that the direct link between the source node and the IoT edge node is not available due to obstacles as shown in Fig. 1. In order to establish the source-IoT node connection, the position of the relay node is determined such as the LoS between the source and the relay node exists. The source node transmits an information signal, while the relay decodes and forwards it to the IoT edge node. The relay node does not have its own power supply and it harvests RF energy from a source based on the time-switching scheme. The piece-wise nonlinear model of energy harvesting is used due to nonlinearities of energy harvesting circuits [20]. Therefore, the saturation effects are incorporated in our model.

The source node transmits the signal s with the power P_S to the relay node. The signal at the relay node can be described as follows:

$$y_R = \sqrt{\frac{P_S}{d_1^{\delta}}} h_{SR} s + n_R , \tag{1}$$

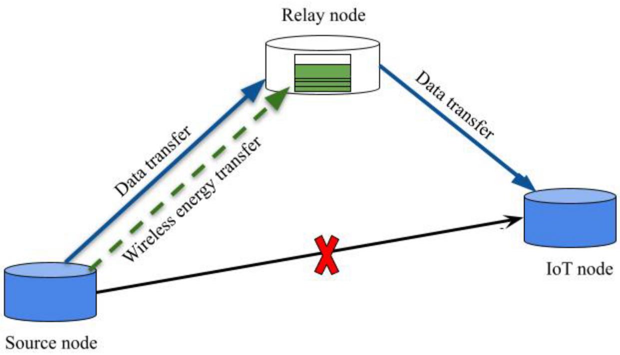

Fig. 1 System model.

where h_{SR} is the fading envelope of the source-to-relay channel, δ is the path loss exponent, d_1 is the distance from the source to the relay node and n_R is the additive white Gaussian noise (AWGN) component at the relay node with the power σ_R^2. The received signal-to-noise ratio (SNR) at the relay node is defined as

$$\gamma_R = \frac{P_S}{d_1^{\delta} \sigma_R^2} \gamma_1 = c_1 \gamma_1 , \tag{2}$$

where $\gamma_1 = |h_{SR}|^2$ is the channel power gain of the source-to-relay link and $c_1 = \frac{P_S}{d_1^{\delta} \sigma_R^2}$.

According to the TSR protocol [10], the first part αT ($0 \le \alpha \le 1$) of each time frame interval of duration T is utilized to harvest the energy required for relay signal transmission, which is equal to

$$E_H = \eta \frac{P_S \gamma_1}{d_1^{\delta}} \alpha T , \tag{3}$$

where η is the energy conversion efficiency coefficient. The rest of the time $(1-\alpha)T$ is used for information transmission, which is divided into two equal parts: the first portion involves sending an information signal to the relay device, and the second part involves sending the information signal from the relay to the IoT edge device, as shown in Fig. 2.

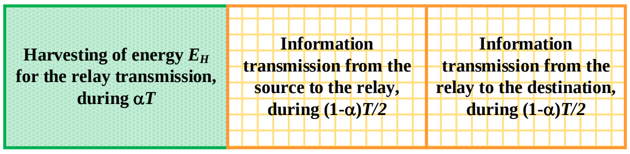

Fig. 2 TSR protocol [21]

We apply the piece-wise nonlinear model under the assumption that the energy harvesting equipment is nonlinear. According to this nonlinearity model, the harvested energy is linearly proportional to the input power for values below the saturation threshold power, P_{th} [20]. A further increase in the input power does not lead to an additional increase of the output power, as the saturation effect occurs. It is assumed that the entire harvested energy is used for information transmission from the relay node. Therefore, the relay transmit power is equal [21]

$$P_R = \frac{E_{\mathrm{H}}}{(1-\alpha)T/2} = \begin{cases} \dfrac{2\eta\alpha}{(1-\alpha)} \dfrac{P_S}{d_1^{\delta}} \gamma_1, & \dfrac{P_S}{d_1^{\delta}} \gamma_1 \le P_{\mathrm{th}}, \\ \dfrac{2\eta\alpha}{1-\alpha} P_{\mathrm{th}}, & \dfrac{P_S}{d_1^{\delta}} \gamma_1 > P_{\mathrm{th}}. \end{cases} \tag{4}$$

The received signal at the IoT edge device can be expressed as

$$y_D = \sqrt{\frac{P_R}{d_2^{\delta}}} h_{RD} s_R + n_D , \tag{5}$$

where h_{RD} is the fading envelope of the relay-to-IoT channel, d_2 is the distance from the relay to the IoT node and n_D is the AWGN component at the IoT node with the power σ_D^2. Denoting the channel power gain of the relay-to-IoT node link as $\gamma_1 = |h_{SR}|^2$, the received SNR at the IoT edge node can be expressed as

$$\gamma_D = P_{\mathrm{R}} \frac{\gamma_2}{d_2^{\delta} \sigma_D^2} = \begin{cases} c_1 c_2 \gamma_1 \gamma_2, & \gamma_1 \le \Gamma, \\ c_1 c_2 \Gamma \gamma_2, & \gamma_1 > \Gamma, \end{cases} \tag{6}$$

with coefficients $c_2 = \dfrac{2\eta\alpha\sigma_R^2}{(1-\alpha)\sigma_D^2 d_2^{\delta}}$ and $\Gamma = \dfrac{P_{\mathrm{th}} d_1^{\delta}}{P_S}$.

2.1. Channel between the source and the relay node

We assume that the relay location enables signal propagation with the LoS component between the source and the relay node. Under this assumption, the statistics of the signal envelope over the source-to-relay channel can be modelled by the Rician distribution [22]. The probability density function (PDF) of the instantaneous channel power gain $\gamma_1 = |h_{SR}|^2$ at the relay node is [22]

$$p_{\gamma_1}(\gamma) = \frac{(K+1)e^{-K}}{\bar{\gamma}_1} e^{-\frac{(K+1)\gamma}{\bar{\gamma}_1}} I_0\left(2\sqrt{\frac{K(K+1)\gamma}{\bar{\gamma}_1}}\right), \tag{7}$$

where K denotes the Rician K factor (equal to the ratio of the power of the LoS component to the average power of the scattered component), $\bar{\gamma}_1 = E[\gamma_1]$ is the average channel power gain at the relay and $I_0(x)$ is the zero-th order modified Bessel function of the first kind [23].

The corresponding cumulative distribution function (CDF) is given by [22]

$$F_{\gamma_1}(\gamma) = 1 - Q\left(\sqrt{2K}, \sqrt{\frac{2(1+K)\gamma}{\bar{\gamma}_1}}\right), \tag{8}$$

where $Q(x)$ is the first-order Marcum Q-function [22].

2.2. Channel between relay and IoT edge node

The IoT node is in the area full of obstacles and it can be considered that in addition to fading in the channel, the shadowing effect occurs. The phenomenon of multipath fading as well as the variation of the average power (as a result of the shadowing effect) are taken into account, so the PDF of the relay-to-IoT node channel gain can be described by composite generalized K distribution

$$p_{\gamma_2}(\gamma) = \frac{2}{\Gamma(m_m)\Gamma(m_s)}\left(\frac{m_m m_s}{\bar{\gamma}_2}\right)^{\frac{m_m+m_s}{2}} \gamma^{\frac{m_m+m_s}{2}-1} K_{m_s-m_m}\left(2\sqrt{\frac{m_m m_s}{\bar{\gamma}_2}\gamma}\right), \tag{9}$$

where m_m is the multipath fading parameter, m_s is the shadowing parameter, $\bar{\gamma}_2 = E[\gamma_2]$ is the average SNR and $K_\mu(x)$ is the modified Bessel function of the second kind [23]. The corresponding CDF is

$$F_{\gamma_2}(\gamma) = \frac{1}{\Gamma(m_m)\Gamma(m_s)} G_{1,3}^{2,1}\left(\frac{m_m m_s \gamma}{\bar{\gamma}_2}\middle| \begin{matrix} 1 \\ m_s, m_m, 0 \end{matrix}\right). \tag{10}$$

where $G_{m,n}^{p,q}\left(x\middle|\begin{matrix} a_r \\ b_s \end{matrix}\right)$ is the Meijer G-function [23].

3. Outage Analysis

The outage probability and the outage capacity of the communication system are important system performance measures. In the considered IoT system with the energy harvesting relay node, if the received SNR at the relay or destination node is less than the predefined threshold, γ_{th}, the system is considered as to be in outage. In that case, the IoT edge node does not have the required quality of service.

Therefore, the probability of system outage is defined as

$$F_{eq}\left(\gamma_{th}\right)=P_{out}=\Pr\left\{\gamma_R\le\gamma_{th}\right\}+\Pr\left\{\gamma_R>\gamma_{th},\gamma_D\le\gamma_{th}\right\}, \tag{11}$$

where Pr{·} denotes the corresponding probability. According to equation (11) and using [24], the outage probability can be calculated as [21]

$$\begin{aligned}F_{eq}\left(\gamma_{th}\right)=&F_{\gamma_1}\left(\frac{\gamma_{th}}{c_1}\right)+\int_{\frac{\gamma_{th}}{c_1}}^{\Gamma}F_{\gamma_2}\left(\frac{\gamma_{th}}{c_1c_2\gamma_1}\right)p_{\gamma_1}\left(\gamma_1\right)d\gamma_1\\&+F_{\gamma_2}\left(\frac{\gamma_{th}}{c_1c_2\Gamma}\right)\left[1-F_{\gamma_1}\left(\max\left(\Gamma,\frac{\gamma_{th}}{c_1}\right)\right)\right],\end{aligned} \tag{12}$$

where the PDF and the CDF expressions for the channel power gain of the source-to-relay node link are defined by (7) and (8), respectively, and CDF for the relay-to-IoT link is given by (10). Substituting corresponding PDF and CDF in the form of special functions in (12) does not lead to the closed-form expression for outage probability. Therefore, the results are obtained by numerical integration and by simulation.

In addition to the outage probability of the system, another important performance metric is the outage capacity. The outage capacity is defined as the maximum data rate that can be achieved in the channel, with the outage probability $F_{eq}(\gamma_{th})$. The outage capacity is given by [25]

$$C_{out}=\frac{1}{2\ln 2}\left(1-F_{eq}\left(\gamma_{th}\right)\right)\ln\left(1+\gamma_{th}\right). \tag{13}$$

Based on the TSR protocol (Fig. 2), the effective time for information transfer from the source node to the IoT node (with the help of the relay node) during the time period of duration T is equal to $(1-\alpha)T$ and the corresponding achievable throughput is given by

$$T_{out}=\left(1-\alpha\right)C_{out}. \tag{14}$$

4. NUMERICAL RESULTS AND DISCUSSION

In this Section, outage performance is analyzed and numerical results are presented and confirmed by the independent Monte-Carlo simulation method. We analyzed the impact of the system and channel parameters on the outage probability and throughput, based on the outage capacity of the considered system with the nonlinear energy harvesting relay node. The simulation is done in MATLAB using 10^7 samples of the fading envelope for both links. For the source-to-relay node samples are generated to follow the Rician distribution, while for the relay-to-IoT node the generated samples appertain generalized K distribution. The system performances are evaluated by averaging over successive channel realizations. The system and channel parameter values used for all presented figures are the following: η=0.8, $\sigma_R^2=\sigma_D^2=0.01$ mW, δ=2 and $\overline{\gamma}_1=\overline{\gamma}_2=1$.

In Fig. 3 the effect of the distance between the source and relay nodes on the outage performance is presented for various values of threshold power P_{th}. With the increase in threshold power values, the outage probability decreases. The effect of threshold power on the quality of service at the IoT node is evident in the whole range of distances. However, when the relay is closer to the source node this impact is more significant. In the case of a linear harvester ($P_{th} \to \infty$), the best performance is obtained by placing the relay as close as possible to the source. At larger distances d_1, the collected power on the relay decreases with the distance, so the harvester does not enter saturation range and nonlinearity does not have an effect on the system performance.

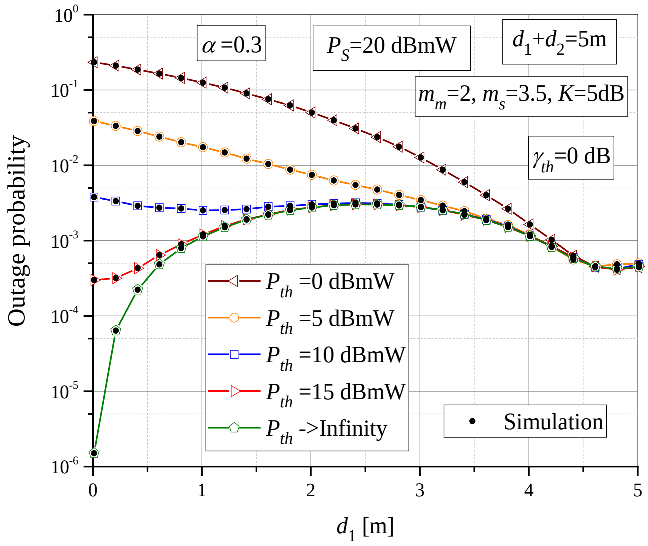

Fig. 3 Outage probability versus source-relay node distance d_1 for various values of threshold power.

The dependence of outage performance on the threshold power is shown in Fig. 4, for various values of the Rician K factor and time-switching coefficient α. For small values of threshold power (P_{th} <-5dBmW), the Rician factor K does not have a significant impact on the outage performance. With the increase of the factor K, the LoS component is more dominant, the outage probability decreases, and the outage floor appears for larger values of the threshold power. The saturation values of outage probability are a function of K. The value of the outage floor depends on the energy harvesting ratio, i.e. time-switching coefficient.

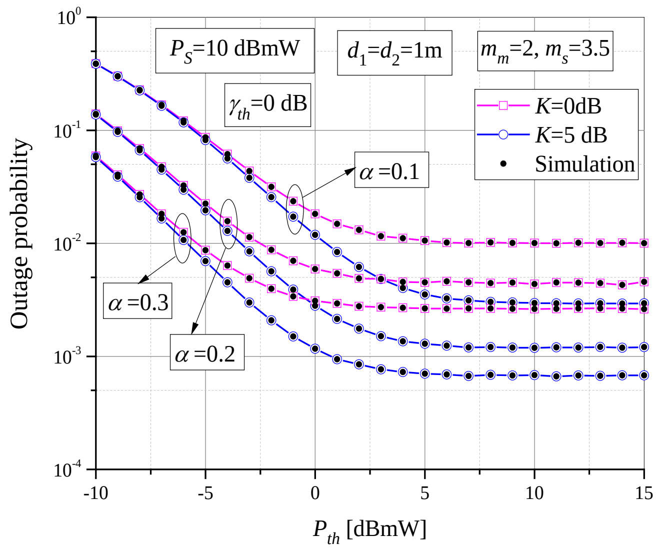

Fig. 4 Outage probability versus threshold power for various values of the Rician K factor and time-switching coefficient.

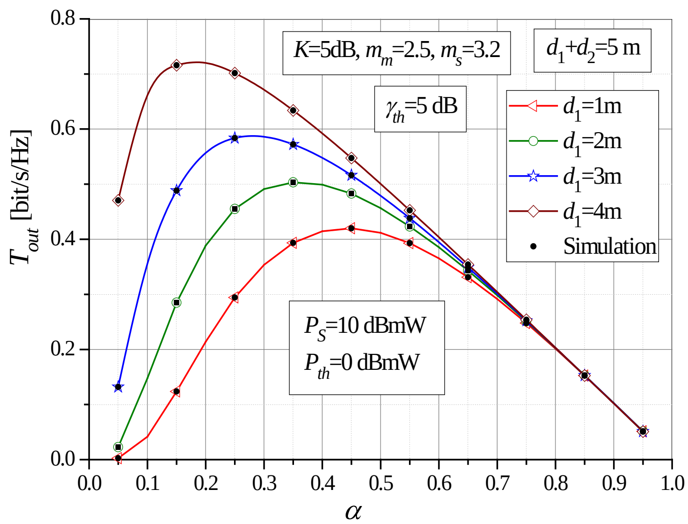

Fig. 5 The throughput T_{out} versus time-switching coefficient for various relay distance from the source, d_1.

In Fig. 5 the dependence of the throughput T_{out} on the time-switching coefficient α is presented for different threshold power values. The sum of the distances on the first and the second link is constant, d_1+d_2=5m. The source node transmits a signal with a power equal P_S=10dBmW, while the value of the saturation threshold due to nonlinearity is

P_{th}=0dBmW. Based on the obtained results, for the considered system parameters, higher throughput values are obtained in the case when the distance between the relay and the IoT node is smaller. This phenomenon can be explained by the fact that in the case of small distances on the first hop, the limitation of the nonlinear device dominantly determines the maximum power of the relay. Also, in that case, the distance between the relay and the IoT node is greater, which reduces the received signal power. It can be observed that the optimal percentage of time dedicated to energy harvesting, which leads to the maximum throughput, decreases with the increase in the source-relay distance.

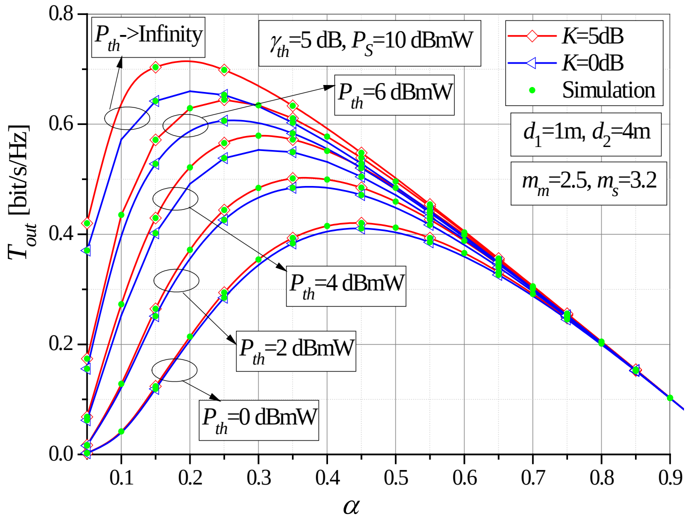

Fig. 6 The throughput T_{out} versus time-switching coefficient α, for various values of the Rician K factor and threshold power.

The throughput T_{out} versus time-switching coefficient α is given in Fig. 6, for various values of the Rician K factor and threshold power, for distances d_1=1m and d_2=4m. In the case when the effect of the energy harvesting relay nonlinearity is dominant, the throughput is significantly reduced. The throughput can be raised by increasing the Rician K factor. The influence of the LoS component is greater when the threshold power is higher. The optimal time-switching coefficient that achieves the maximum throughput increases with the decrease of threshold power.

The dependence of throughput T_{out} on the saturation threshold power P_{th} is shown in Fig. 7, for different fading and shadowing conditions of the relay-to-IoT channel, as well as for different percentage of relay charging within time frame. As the value of the saturation threshold increases, the performance improves, but above a certain value of P_{th}, the system achieves saturation that corresponds to the performance in the case when the harvester is linear. Higher values of the fading and shadowing parameters correspond to the better channel conditions, so the throughput also have increased values. At lower threshold power values, the throughput increases with the increase of time-switching coefficient value, which can also be seen in Fig. 6 observing the optimal time-switching value achieving maximum throughput. When nonlinearity of the harvester is not a limiting factor, better performances are obtained with a smaller time-switching coefficient value due to the increase in the time dedicated to signal transmission.

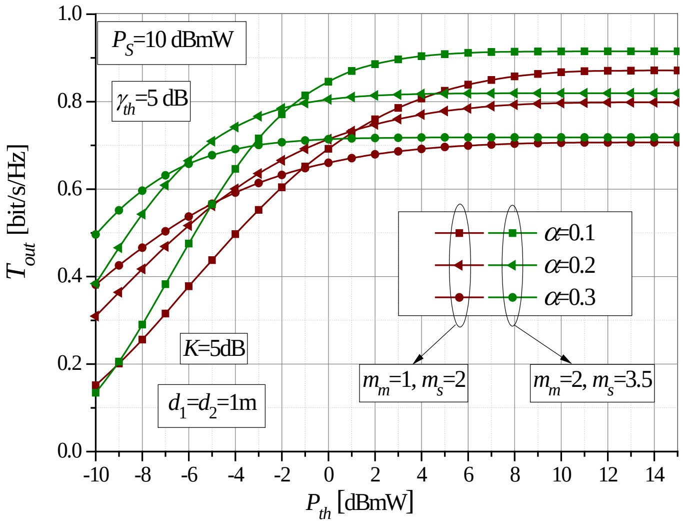

Fig. 7 The throughput T_{out} versus threshold power, for various values of time-switching coefficient α and various values of the relay-IoT channel parameters.

5. CONCLUSION

Improving the energy efficiency of the IoT system is possible by applying energy harvesting technology, which involves collecting the existing energy from the environment. Apart from the natural energy sources, RF signals and existing interference from the RF range can also be used as energy sources, enabling simultaneous transmission of energy and information. For this reason, there is a great interest in the application of energy harvesting technology in modern concepts and networks where energy efficiency is a major challenge, such as IoT and 5G networks.

In this paper we analyzed an IoT system where the relay node was supplied by RF energy from the source node and establishes information transfer from the source to the IoT edge node. The relay position was determined such that LoS was provided between the source and the relay nodes, and the channel gain was modeled by the Rician distribution. The relay-IoT edge node link was influenced by the simultaneous existence of multipath fading and shadowing effects, which were modeled by the Generalized-K distribution. The analytical and simulation numerical results were obtained for the outage performance metrics and the excellent agreement between results was obtained by using both of the observed approaches. The impact of nonlinearity in the energy harvester, system and channel parameters on the system performances was discussed. We also examined the influence of the relay position as well as the charging time on the throughput and outage probability.

REFERENCES

1. Akin-Ponnle, A.E., Carvalho, N.B., 2021, *Energy harvesting mechanisms in a smart city-A review*, Smart Cities, 4(2), pp. 476-498.
2. Yu, H., Chin, K., Soh, S., 2022, C*harging RF-energy harvesting devices in IoT networks with imperfect CSI*, IEEE Internet of Things Journal, 9(18), pp. 17808-17820.
3. Ku, M.L., Li, W., Chen, Y., Liu, K., 2015, *Advances in energy harvesting communications: past, present, and future challenges*, IEEE Communications Surveys & Tutorials, 18(2), pp. 1384-1412.
4. Ramezani, P., Jamalipour, A., 2017, *Toward the evolution of wireless powered communication networks for the future Internet of things*, IEEE Network, 31(6), pp. 62-69.
5. Zhao, N., Zhang, S., Yu, F.R., Chen, Y., Nallanathan, A., Leung, V.C.M., 2017, *Exploiting interference for energy harvesting: a survey, research issues and challenges*, IEEE Access, 5, pp. 10403-10421.
6. Bapatla, D., Prakriya, S., 2021, *Performance of Two-Hop Links With an Energy Buffer-Aided IoT Source and a Data Buffer-Aided Relay*, IEEE Internet of Things Journal, 8(6), pp. 5045-5061.
7. Toan, V.H., Hoang, T.M., Dũng, L.T., 2020, *Outage probability analysis of decode-and-forward two-way relaying system with energy harvesting relay*, Wireless Communications and Mobile Computing, 2020, pp. 1530-8669.
8. Varshney, L., 2008, *Transporting information and energy simultaneously*, IEEE International Symposium on Information Theory - Proceedings, pp. 1612-1616.
9. Liu, L., Zhang, R., Chua, K.C., 2012, *Wireless information transfer with opportunistic energy harvesting*, IEEE Transactions on Wireless Communications, 12(1), pp. 288-300.
10. Nasir, A.A., Zhou, X., Durrani, S., Kennedy, R.A., 2012, *Relaying protocols for wireless energy harvesting and information processing*, IEEE Transactions on Wireless Communications, 12(7), pp. 3622-3636.
11. Nasir, A.A., Zhou, X., Durrani, S., Kennedy, R.A., 2014, *Throughput and ergodic capacity of wireless energy harvesting based DF relaying network*, Proc. IEEE International Conference on Communications (ICC), pp. 4066-4071, Sydney, Australia.
12. Chen, Y., 2018, *Energy Harvesting for Wireless Relaying Systems*, Wireless Information and Power Transfer: A New Paradigm for Green Communications, Chapter 5, pp. 123-155.
13. Ding H., da Costa D.B., Wang X., Dias U.S., de Sousa R.T., Ge J., 2016, *On the effects of LOS path and opportunistic scheduling in energy harvesting relay systems*, IEEE Transactions on Wireless Communications, 15(12), pp. 8506-8524.
14. Cvetkovic, A., Blagojevic, V., 2017, *The influence of LOS and shadowing components on outage probability of energy harvesting DF relay system*, Proc. International Scientific Conference on Information, Communication and Energy Systems and Technologies (ICEST), pp. 28-30, Niš, Serbia.
15. Blagojevic, V., Cvetkovic, A., Ivanis, P., 2018, *Performance analysis of energy harvesting DF relay system in generalized-K fading environment*, Physical Communication, 28, pp. 190-200.
16. Boshkovska, E., Ng, D.W.K., Zlatanov, N., Schober, R., 2015, *Practical non-linear energy harvesting model and resource allocation for SWIPT systems*, IEEE Communications Letters, 19(12), pp. 2082-2085.
17. Valenta, C.R. and Durgin, G.D., 2014, *Harvesting wireless power: survey of energy-harvester conversion efficiency in far-field, wireless power transfer systems*, IEEE Microwave Magazine., 15(4), pp. 108-120.
18. Cvetkovic, A., Blagojevic, V., Ivanis, P., 2017, *Performance analysis of nonlinear energy-harvesting DF relay system in interference-limited Nakagami-m Fading Environment*, ETRI Journal, 39(6), pp. 803-812.
19. Zhang, J., Pan, G., 2016, *Outage analysis of wireless-powered relaying MIMO systems with non-linear energy harvesters and imperfect CSI*, IEEE Access, 4, pp. 7046-7053.
20. Dong, Y., Hossain, M.J., Cheng, J., 2016, *Performance of wireless powered amplify and forward relaying over Nakagami-m fading channels with nonlinear energy harvester*, IEEE Communications Letters, 20(4), pp. 672-675.
21. Blagojevic, V., Cvetkovic, A., Ivanis, P., 2018, *On the capacity of SWIPT cooperative relaying system in generalized fading environment*, Proc. International Conference on Systems, Automatic Control and Measurements (SAUM), Niš, Serbia.
22. Simon, M., Alouini, M.S., 2005, *Digital Communications Over Fading Channels: A Unified Approach to Performance Analysis*, 2th edition, John Wiley & Sons, New York, NY, USA, 544 p.
23. Gradshteyn, I.S., Ryzhik, I.M., 2007, *Table of Integrals, Series, and Products*, 7th edition, San Diego, CA, USA, 1200 p.
24. Papoulis, A., 1991, *Probability, Random Variables, and Stochastic Processes*, New York, USA: McGraw-Hill, 852 p.
25. Gu, Y., Aıssa, S., 2015, *RF-based energy harvesting in decode-and-forward relaying systems: ergodic and outage capacities*, IEEE Transactions on Wireless Communications, 14(11), pp. 6425–6434.